



## A Saturated Red-Emitting Phosphorescent Iridium(III) Complex for Application in Organic Light Emitting Diodes

Liyang Zhang,<sup>a,b</sup> Bin Li,<sup>a,z</sup> Liming Zhang,<sup>a</sup> Shumei Yue, Qin Xue,<sup>c</sup> and Shiyong Liu<sup>c,z</sup>

<sup>a</sup>Key Laboratory of Excited State Processes, Changchun Institute of Optics, Fine Mechanics and Physics, Changchun 130033, People's Republic of China

<sup>b</sup>College of Science, Henan University of Technology, Zhengzhou 450001, People's Republic of China

<sup>c</sup>State key Lab of Integrated Optoelectronics, Jilin University, Changchun 130023, People's Republic of China

A novel ancillary ligand (2-(1-hydroxy-naphthyl)-benzothiazolato) (HNBT) and corresponding iridium(III) complex, Ir(ppy)<sub>2</sub>(NBT) (ppy = 2-phenylpyridine) are synthesized, and red-emitting electrophosphorescent devices by doping Ir(ppy)<sub>2</sub>(NBT) in 4,4'-N,N'-dicarbazole-biphenyl (CBP) are fabricated. The optimized device displays EL spectrum with a narrow full-width at half-maximum of 65 nm, and the Commission International de L'Eclairage (CIE) coordinates of (0.65, 0.33) are very close to those suggested by the National Television System Committee (NTSC) standard for a red emitter.

© 2011 The Electrochemical Society. [DOI: 10.1149/1.3596543] All rights reserved.

Manuscript submitted December 30, 2010; revised manuscript received April 11, 2011. Published June 9, 2011.

Organometallic complexes possessing a heavy transition metal element are crucial for the fabrication of phosphorescent organic light emitting diodes (OLEDs).<sup>1-7</sup> The strong spin-orbit coupling effectively promotes intersystem crossing as well as enhances the subsequent emissive decay from the triplet excited state to the ground state, facilitating strong phosphorescence by harvesting both singlet and triplet excitons. Because an internal quantum efficiency as high as 100% can theoretically be achieved, these heavy-metal containing emitters are superior to their fluorescent counterparts in OLED applications.<sup>1,8</sup>

Iridium-based emitters are considered to be the seminal generation of phosphorescence emitters.<sup>9-11</sup> In most heteroleptic Ir(III) complexes studied in OLEDs so far, the effort have been focused on changing the structure of the cyclometalating ligand because both the efficiency and emission wavelength of the electroluminescence (EL) are strongly dependent on its choice, while in most cases the auxiliary ligand is the acetylacetonate anion, and highly efficient OLEDs using Ir(III) complexes with emission covering the whole visible region have been realized by this method.<sup>12-16</sup> Researchers from Xie et al. have reported red-light-emitting iridium complexes for electrophosphorescence color purity trade-off optimization.<sup>17</sup> However, these devices based on the Ir(III) complexes as emitters generally have relatively broad bands, which is not well-suited for actual display application. Investigation about tuning the color purity by decreasing the emission bandwidth which is attractive for both fundamental research and practical applications, is rare,<sup>18</sup> and the relative research about red Ir(III) complexes has not been reported. In this paper, we first report a novel red Ir(III) complex with narrow emission bandwidth, bis(2-phenylpyridine)-iridium(1-benzo[b]thiophen-2-yl-naphthalene-2-ol) [Ir(ppy)<sub>2</sub>(NBT)] using a phenol derivative HNBT as ancillary ligand. Saturated red EL devices are fabricated by doping Ir(ppy)<sub>2</sub>(NBT) in 4,4'-N,N'-dicarbazole-biphenyl (CBP). The optimized device exhibits a maximum brightness of 6400 cd/m<sup>2</sup> and the peak current efficiency is 4.53 cd/A. It is noteworthy that the device displays narrow EL spectrum originated from Ir(III) complex Ir(ppy)<sub>2</sub>(NBT) with a full-width at half-maximum (FWHM) of 65 nm and the Commission International de L'Eclairage (CIE) coordinates of (0.65, 0.33).

The new ligand HNBT, and the corresponding complex Ir(ppy)<sub>2</sub>(NBT), were synthesized separately according to literature procedures.<sup>19,20</sup> Both ligand and complex were characterized by <sup>1</sup>H NMR, IR, and elemental analysis. The highest occupied molecular orbital (HOMO) and the lowest unoccupied molecular orbital (LUMO) energy levels of Ir(ppy)<sub>2</sub>(NBT) were determined by cyclic voltammetry. The photoluminescence (PL) decay of Ir(ppy)<sub>2</sub>(NBT) in solid films were measured by a quanta ray DCR-3 pulsed Nd: YAG laser system under excitation of 355 nm laser pulse. The multilayer devices

of ITO/NPB (30 nm)/wt % Ir(ppy)<sub>2</sub>(NBT) doped in CBP (30 nm)/BCP (10 nm)/Alq<sub>3</sub> (30 nm)/LiF (0.8 nm)/Al were made by successive thermal evaporation of organic materials and metal electrode material in high vacuum ( $\leq 8 \times 10^{-5}$  Pa) onto precleaned ITO substrate. EL spectra of these devices were measured by a PR650 spectrascan spectrometer. The luminance-current density-voltage characteristics were recorded simultaneously with the measurement of EL spectra by combining the spectrometer with a Keithley 2400 source meter. All measurements were carried out in air at room temperature.

The absorption and emission spectra of complex Ir(ppy)<sub>2</sub>(NBT) in dichloromethane solution with the concentration  $1.0 \times 10^{-4}$  mol/l at 298 K are shown in Fig. 1. Intense multiple absorption bands appearing in the ultraviolet part of the spectrum between 240 and 360 nm are assigned to the spin-allowed  $\pi-\pi^*$  transitions of the intraligand. The broad weak absorption bands at 360 and 530 nm are assigned to the transitions from the ground state to the singlet metal-ligand-charge-transfer (<sup>1</sup>MLCT) and triplet MLCT (<sup>3</sup>MLCT) excited states.<sup>16,21</sup> The intensity of the <sup>3</sup>MLCT transition is close to that of <sup>1</sup>MLCT, suggesting that the <sup>3</sup>MLCT transition is strongly allowed by an effective mixing of singlet-triplet with higher lying spin-allowed transitions on the cyclometalated ligand.<sup>22</sup> This mixing is facilitated by the strong spin-orbit coupling of the Ir(III) center. The emission spectrum of Ir(ppy)<sub>2</sub>(NBT) exhibits a perfect gauss like band shape centering at 614 nm with a narrow FWHM of 65 nm, so we presume that the excited state is dominated by one species, which can be confirmed by the excited state decay, which is shown in Fig. 2. The

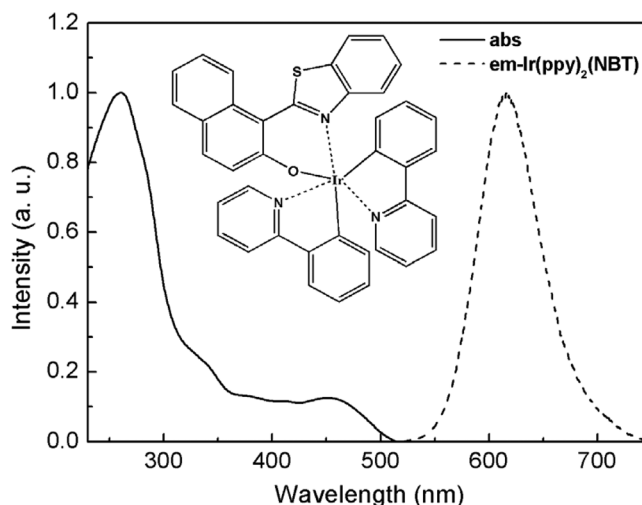


**Figure 1.** Absorption and emission spectra of complex Ir(ppy)<sub>2</sub>(NBT) in dichloromethane solution with the concentration  $1.0 \times 10^{-4}$  mol/l. Inset: the chemical structure of Ir(ppy)<sub>2</sub>(NBT).

<sup>z</sup> E-mail: lib020@ciomp.ac.cn; sylu@mail.jlu.edu.cn

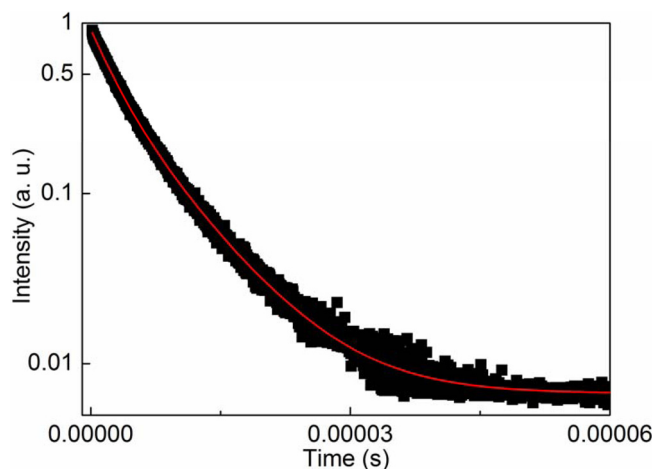


**Figure 2.** (Color online) Photoluminescence lifetime decay of complex  $\text{Ir(ppy)}_2(\text{NBT})$  measured at 77 K.

excited state decay is monoexponential with a lifetime of  $4.7 \mu\text{s}$ , and the phosphorescence quantum yield of  $\text{Ir(ppy)}_2(\text{NBT})$  is 0.25. Otherwise, thermal stability is investigated by TGA, and its 5% decomposition temperature is  $317^\circ\text{C}$ .

To investigate EL properties of  $\text{Ir(ppy)}_2(\text{NBT})$ , several devices using on  $\text{Ir(ppy)}_2(\text{NBT})$  as dopant and CBP as host were fabricated. First, four multilayer devices with the configuration of ITO/NPB (30 nm)/ $\times$  wt %  $\text{Ir(ppy)}_2(\text{NBT})$  doped in CBP (30 nm)/BCP (10 nm)/ $\text{Alq}_3$  (30 nm)/LiF (0.8 nm)/Al were fabricated. NPB is the hole-transporting, and meanwhile BCP and  $\text{Alq}_3$  are employed as the hole-blocking layer and the electron-transporting layer, respectively. To optimize the device efficiency, a concentration dependence experiment was carried out in a range between 2–10 wt %. As in the case of other phosphorescent OLEDs, the device performances show a strong dependence on the doping concentration. Comparison of performance of these four devices suggests that the device with 8 wt %  $\text{Ir(ppy)}_2(\text{NBT})$  in CBP offers the highest device efficiency. A maximum brightness of  $3652 \text{ cd/m}^2$  at a current density of  $372 \text{ mA/cm}^2$  with voltage of 15.5 V and a maximum current efficiency of  $2.10 \text{ cd/A}$  at a current of  $3.26 \text{ mA/cm}^2$  with the luminance of  $55 \text{ cd/m}^2$  were achieved. Unfortunately, from the EL spectra of these devices, except for red emission centered at 614 nm, the EL spectra of these devices at 17 V exhibit blue emission at 440 nm from NPB, resulting from electron leakage from the doped CBP layer into the hole-transporting layer. So in order to confine excitons recombination zone in emission layer, we insert an electron-blocking layer Irppz between hole-transporting layer and emission layer with thickness of 5 nm, and the

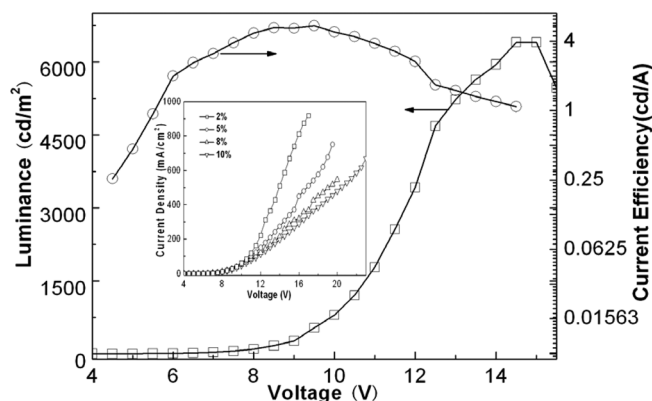


**Figure 3.** Current efficiency-luminance-voltage characteristics of the Irppz based device. Inset: The current-density vs voltage characteristics of the EL devices.

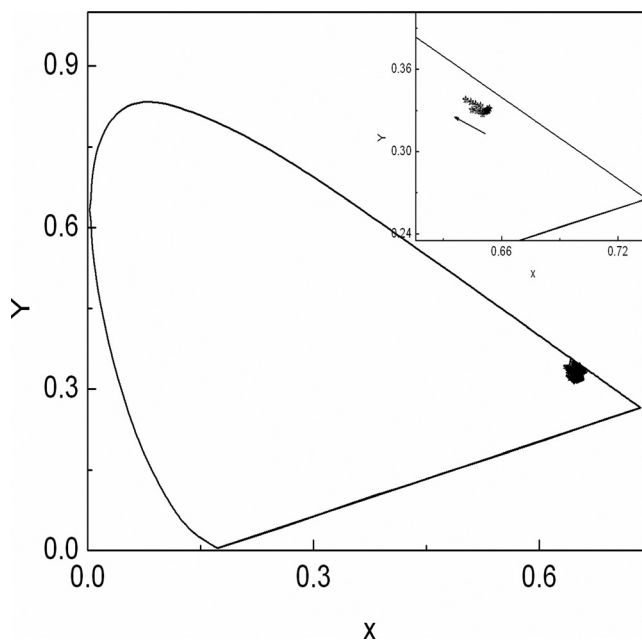


**Figure 4.** CIE coordinates of the Irppz based device. The arrow indicates increasing voltages from 5 to 15.5 V.

concentration of  $\text{Ir(ppy)}_2(\text{NBT})$  is 8 wt %. The insertion of an electron-blocking layer  $\text{Ir(ppz)}_3$  leads to both improved color purity and quantum efficiency. The Irppz based device displays saturated red emission which is consistent with the PL spectrum and no NPB emission is observed at any bias level, indicating the electron leakage into the NPB layer is eliminated. Figure 3 displays the luminance-voltage-efficiency characteristics. The peak brightness is  $6400 \text{ cd/m}^2$  at 15 V and the maximum current efficiency is  $4.53 \text{ cd/A}$  with the CIE coordinates of (0.65, 0.33) at  $11.7 \text{ mA/cm}^2$ . The efficiency of the device with an Irppz blocking layer is double that of the device without Irppz blocking layer. Figure 4 shows the CIE coordinates from 5 to 15.5 V. We can see that the CIE coordinates are fairly stable over a range of operation voltages and the region is just around the standard red point, although there is some small shift in the inset, which might be caused by the detrapping process of dopant excitons or excitons' quenching at high current density.

We also discussed the mechanism of the EL device. The considerable overlap between the PL spectrum of CBP and the absorption of  $\text{Ir(ppy)}_2(\text{NBT})$ , as shown in Fig. 5, indicates that Förster energy

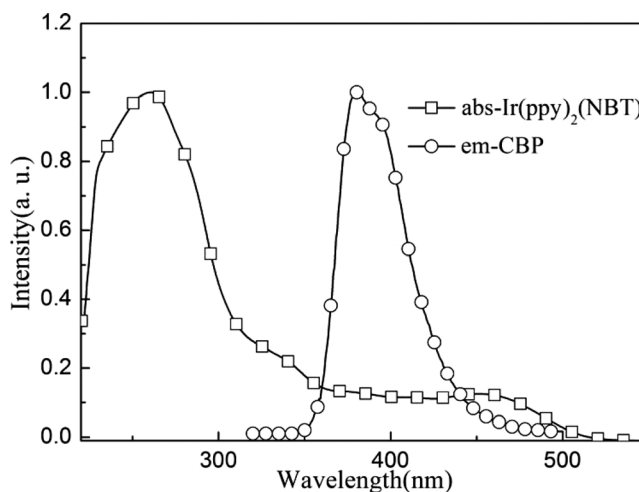


**Figure 5.** Absorption and emission spectra of  $\text{CBP:Ir(ppy)}_2(\text{NBT})$  film.

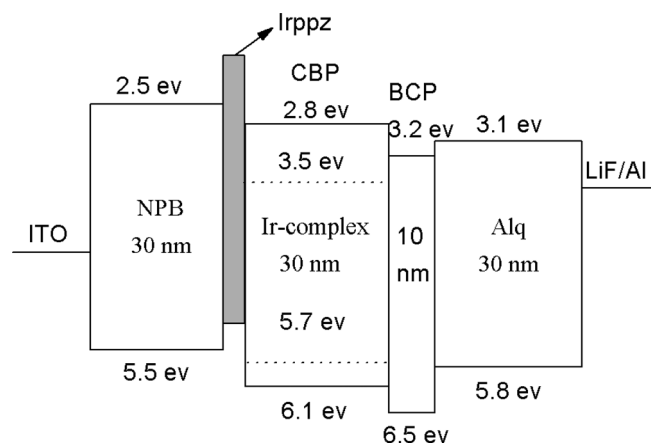


Figure 6. The proposed energy level diagram of the devices.

transfer from the singlet in CBP host to the MLCT state of  $\text{Ir(ppy)}_2(\text{NBT})$  is possible. On the other hand, Fig. 6 shows the proposed energy level diagram of the devices, according to the energy level alignment, the charge trapping mechanism is favorable, since the HOMO and LUMO levels of  $\text{Ir(ppy)}_2(\text{NBT})$  are 5.7 and 3.5 eV, respectively, lying between the band gap of CBP, which meets the requirement for efficient carrier trapping.<sup>23</sup> The LUMO of  $\text{Ir(ppy)}_2(\text{NBT})$ , 0.7 eV higher than that of CBP, may behave as deep electron traps in CBP, enabling effective electron trapping therein. Its HOMO level which is 0.4 eV lower than CBP also eases hole injection from NPB to CBP. So the direct charge trapping is likely the dominant process in the EL devices. Meanwhile, efficient charge-trapping of complex  $\text{Ir(ppy)}_2(\text{NBT})$  is supported by the current-density vs voltage ( $J$ - $V$ ) characteristics of the EL devices based on  $\text{Ir(ppy)}_2(\text{NBT})$  with different doping levels, which are shown in the inset of Fig. 3. We can see that the  $J$ - $V$  characteristic curves shift gradually to higher voltage with increasing doping concentration, suggesting that the trapping effect of the  $\text{Ir(ppy)}_2(\text{NBT})$  basically decrease the carrier transport mobility. Furthermore, the emissive intensity of NPB is also a direct evidence for charge trapping mechanism. Since hole injection from the NPB HOMO into the CBP HOMO is energetically unfavourable, so when the dopant concentration is low, accumulated holes in NPB layer can recombine with the electrons injected from the emissive layer, resulting in NPB emission in addition to exciton formation at  $\text{Ir(ppy)}_2(\text{NBT})$ . With increasing doping concentrations, more and more electrons can be intercepted and trapped by  $\text{Ir(ppy)}_2(\text{NBT})$  and the contribution from NPB decreased. In a word, Förster energy transfer and charge-trapping of complex  $\text{Ir(ppy)}_2(\text{NBT})$  should be responsible for the good electrophosphorescent performances. Also, when the voltage is low, the traps are not filled completely, and the concentration of  $\text{Ir(ppy)}_2(\text{NBT})$  has little effect on the  $J$ - $V$  curves of the devices. As increasing of voltage, more and more electrons are injected, the traps of the device with low dopant concentration are filled, while the device with high dopant concentration has more sites to trap. So from inset of Fig. 3,  $J$ - $V$  curves seem to be close at low voltage (under 10 V) and differ a lot with increasing driving voltage ( $>12$  V).

In summary, We firstly synthesized a highly efficient pure red-emitting Ir(III) complex of  $\text{Ir(ppy)}_2(\text{NBT})$ , and EL devices were also fabricated. The optimized EL device possesses a maximum brightness of 6400 cd/m<sup>2</sup> and the peak current efficiency of 4.53 cd/A, and emits saturated red light with CIE coordinates of (0.65, 0.33) which is very close to the perfect red desired for display and illumination applications. More importantly, narrowing emissive bandwidth of electrophosphorescent Ir(III) complex is realized by simply utilizing a phenol derivative as ancillary ligand. This work, therefore, opens the door to tuning the color purity of phosphorescent complexes by using phenol derivative as ligand.

### Acknowledgments

The authors gratefully thank the financial supports of the National Natural Science Foundations of China (Grant Nos. 50872130 and 21041007) and the Science and Technology Developing Project of Jilin Province (Grant No. 20100533).

### References

1. M. A. Baldo, D. F. O'Brien, Y. You, A. Shoustikov, S. Sibley, M. E. Thompson, and S. R. Forrest, *Nature (London)*, **395**, 151 (1998).
2. M. A. Baldo, M. E. Thompson, and S. R. Forrest, *Pure Appl. Chem.*, **71**, 2095 (1999).
3. A. S. Ionkin, W. J. Marshall, and Y. Wang, *Organometallics*, **24**, 619 (2005).
4. P. T. Furuta, L. Deng, S. Garon, M. E. Thompson, and J. M. J. Frechet, *J. Am. Chem. Soc.*, **126**, 15388 (2004).
5. W. Sotoyama, T. Satoh, N. Sawatari, and H. Inoue, *Appl. Phys. Lett.*, **88**, 153505 (2005).
6. M. A. Baldo, S. Lamandky, P. E. Burrows, M. E. Thompson, and S. R. Forrest, *Appl. Phys. Lett.*, **75**, 4 (1999).
7. F. Babudri, G. M. Farinola, F. Naso, and R. Ragni, *Chem. Commun.*, 1003 (2007).
8. C. Adachi, M. A. Baldo, S. R. Forrest, S. Lamansky, M. E. Thompson, and R. C. Kwong, *Appl. Phys. Lett.*, **78**, 1622 (2001).
9. H. Y. Chen, Y. Chi, C. S. Liu, J. K. Yu, Y. M. Cheng, K. S. Chen, P. T. Chou, S. M. Peng, G. H. Lee, A. J. Carty et al., *Adv. Funct. Mater.*, **15**, 567 (2005).
10. M. S. Lowry and S. Bernhard, *Chem. Eur. J.*, **12**, 7970 (2006).
11. E. M. Hwang, H. Y. Chen, P. S. Chen, C. S. Liu, C. F. Shu, E. L. Wu, P. T. Chou, S. M. Peng and G. H. Lee, *Inorg. Chem.*, **44**, 1344 (2005).
12. J. P. Duan, P. P. Sun, and C. H. Cheng, *Adv. Mater.*, **15**, 224 (2003).
13. C. H. Yang, C. C. Tai, and I. W. Sun, *J. Mater. Chem.*, **14**, 947 (2004).
14. X. W. Chen, J. L. Liao, Y. M. Liang, M. O. Ahmed, H. E. Seng, and S. A. Chen, *J. Am. Chem. Soc.*, **125**, 636 (2003).
15. W. S. Huang, J. T. Lin, C. H. Chien, Y. T. Tao, S. S. Sun, and Y. S. Wen, *Chem. Mater.*, **16**, 2480 (2004).
16. S. Lamansky, P. Djurovich, D. Murphy, F. Abdel-Razzaq, H.-E. Lee, C. Adachi, P. E. Burrows, S. R. Forrest, and M. E. Thompson, *J. Am. Chem. Soc.*, **123**, 4304 (2001).
17. C. L. Ho, W. Y. Wong, Z. Q. Gao, C. H. Chen, K. W. Cheah, B. Yao, Z. Y. Xie, Q. Wang, D. G. Ma, L. X. Wang et al., *Adv. Funct. Mater.*, **18**, 319 (2008).
18. H. J. Bolink, E. Coronado, S. G. Santamarira, M. Sessolo, N. Evans, C. Klein, E. Baranoff, K. Kalyanasundaram, M. Graetzel, and M. K. Nazeeruddin, *Chem. Commun.*, 3276 (2007).
19. W. C. Chang, A. T. Hu, J. P. Duan, D. K. Rayabarapu, and C. H. Cheng, *J. Organomet. Chem.*, **689**, 4882 (2004).
20. S. Kappaun, S. Sax, S. Eder, K. C. Miller, K. Waich, F. Niedermair, R. Saf, K. Merz, J. Jacob, K. Millen et al., *Chem. Mater.*, **19**, 1209 (2007).
21. C. Schaffner-Hamann, A. Zelewsky, A. Barbieri, F. Barigelletti, F. Muller, J. P. Riehl, and A. Neels, *J. Am. Chem. Soc.*, **126**, 9339 (2004).
22. S. Lamansky, P. Djurovich, D. Murphy, F. Abdel-Razzaq, H. E. Lee, C. Adachi, P. E. Burrows, S. R. Forrest, and M. E. Thompson, *J. Am. Chem. Soc.*, **123**, 4304 (2001).
23. A. A. Shoustikov, Y. J. You, and M. E. Thompson, *IEEE J. Sel. Top. Quan.*, **4**, 3 (1998).